Available online at www.sciencedirect.com
SCIENCE DIRECT®
Catalysis Today 90 (2004) 115–119
CATALYSIS TODAY
www.elsevier.com/locate/cattod

Kinetic model of indole HDN over molybdenum carbide: influence of potassium on early and late denitrogenation pathways

G. Adamski [a,b], K. Dyrek [a], A. Kotarba [a], Z. Sojka [a,c,*], C. Sayag [b], G. Djéga-Mariadassou [b]

[a] *Faculty of Chemistry, Jagiellonian University, Ingardena 3, 30-060 Cracow, Poland*
[b] *Laboratoire Réactivité de Surface, Université P. et M. Curie, UMR CNRS 7609, casier 178, 4 Place Jussieu 75252 Paris, France*
[c] *Regional Laboratory of Physicochemical Analyses and Structural Research, Jagiellonian University, Ingardena 3, 30-060 Cracow, Poland*

Received 4 September 2003; received in revised form 30 October 2003; accepted 14 November 2003

Available online 11 June 2004

Abstract

Hydrodenitridation of indole over undoped and potassium doped (0.01–1 wt.%) Mo_2C catalysts was studied at 573 K under a pressure of 50 atm and contact times ranging from 0.03 to 0.7 s. The measured concentration profiles of indole, *o*-ethylaniline, ethylcyclohexane and ethylbenzene were successfully analyzed in terms of a kinetic model derived from two doubly coupled cycles, with early and late denitrogenation steps, in the whole range of the investigated contact times. The influence of potassium on the determined rate constants and the selectivity to aromatics vs. cycloparaffines was quantified and briefly discussed.

Keywords: Catalysis; Molybdenum carbide; Indole; Potassium; Promotion; HDN; Kinetic model

1. Introduction

Aromatic nitrogen compounds such as indole, quinoline or carbazole are the main nitrogen-containing components of petroleum. For production of environmentally acceptable fuels they have to be removed in hydrotreating processes, otherwise their burning would lead to air-polluting emission of nitrogen oxides. Hydrodenitrogenation (HDN) apart from hydrodesurfurization (HDS) is one of the biggest petroleum refining processes. Interest in deep hydrodenitrogenation of petroleum has been prompted by arduous environmental regulations.

Among new catalysts active in HDN, carbides of transition metals received a great attention with Mo_2C being the most promising [1]. Insertion of carbon atoms into the lattice of molybdenum leads, due to lattice expansion, to the appearance of a narrower metallic type band with a density of states at the Fermi level similar to that of noble metals [2]. Alkali metals are often used as promoters in industrial processes involving hydrogen. Their beneficial influence on catalyst activity, selectivity and durability in such reactions as ammonia synthesis, water gas shift reaction, Fisher–Tropsch and styrene production is well acknowledged. The impact of potassium on the electronic properties of Mo_2C in relation to the HDN reaction was discussed in our earlier papers [3,4]. In this study the kinetics of HDN of indole over the bare and potassium promoted Mo_2C catalysts was investigated.

2. Experimental

2.1. Preparation and characterization of catalysts

The Mo_2C catalysts were prepared by temperature programmed carburization of MoO_3 precursor. The reaction was carried out under atmospheric pressure in a flow of 10 vol.% CH_4 in H_2 with a gas hourly space velocity GHSV = 68 h^{-1}. The temperature was linearly increased from room temperature to 1023 K with a rate of 53 K h^{-1}. The samples were then kept at these conditions for 1 h, subsequently quenched to room temperature in a flow of helium, and finally passivated with 0.5 cm^3 pulses of O_2 until complete saturation of the surface. Alkali addition can be effected in two main ways: by *nascent-doping* when the promoter is added to the oxide precursor before the carburization reaction and

* Corresponding author. Tel.: +48-12-6336377; fax: +48-12-6340515.
E-mail address: sojka@chemia.uj.edu.pl (Z. Sojka).

0920-5861/$ – see front matter © 2004 Elsevier B.V. All rights reserved.
doi:10.1016/j.cattod.2004.04.015

by *post-doping* when it is added after the synthesis of the final carbide. The first procedure was found to inhibit significantly the carburization process driving the synthesis towards metallic molybdenum [5] and, additionally, only a part of the promoter is present at the external surface. Therefore, in this study potassium promotion was accomplished by the *post-doping* procedure by using a 1:1-K-naphtalene charge transfer complex dissolved in THF. The samples were doped with 0.002, 0.01, 0.05, 0.2 and 1 wt. % of potassium, which correspond to surface coverages (Θ_K) in the range 10^{-3} to 10^{-1} of a monolayer (ML). The surface state of potassium was examined by thermal desorption of K atoms and K^+ ions [3,4]. The influence of potassium on the surface electronic properties of Mo_2C was investigated by measurements of the contact potential difference using the Kelvin dynamic condenser method. Two regions of K promotion were identified: a strong electronic promotion (changes in chemical potential of electrons) at coverage $\Theta_K <\sim 0.05$, and a basic one (changes in surface acid–base properties) for $\Theta_K >\sim 0.05$ [4].

The phase identity of the catalysts was confirmed by XRD measurements (Siemens D500) using the JCPDS 35-0787 database as a reference. In all the synthesized samples only the diffraction pattern characteristic of the compact β-Mo_2C hexagonal phase was observed and the diffraction peaks were indexed within the P63/mmc space group. The morphology and particle size distribution of the molybdenum carbide was examined with a transmission electron microscope (JEOL-JEM 100 CXII). The TEM micrographs showed a uniform morphology of the samples with a average grain size of 100–200 nm. The grains were composed of loosely aggregated small rounded crystallites with an average diameter equal to 17 nm, as derived from the X-ray line broadening using the Debye–Scherrer formula. The BET surface area (Quantachrome) of the investigated samples was in the range of $50 \pm 10\,m^2\,g^{-1}$. The amount of the carbon monoxide chemisorbed was used to determine the number of accessible surface molybdenum atoms, constituting the metallic active sites of the undoped and K-doped Mo_2C catalysts. For the CO-chemisorption measurements pulses of 20 μmol of CO (Air Liquide 99.997%) in flowing He (Air Liquide 99.995%) were injected on the sample every 2 min. The procedure was continued until the surface was completely saturated with CO molecules and the amount of chemisorbed CO was measured by thermal conductivity detector (TCD). The addition of potassium caused a distinct monotonous decrease in the number of surface metallic sites as indicated by the lowering of CO uptake. The results are summarized in Table 1. A more detailed characterization of the investigated catalysts can be found elsewhere [4].

Table 1
Characterization of K-doped Mo_2C catalysts

K content (wt.%)	Surface coverage (ML)	CO uptake ($\mu mol\,g^{-1}$)	Work function changes (eV)
0.0	0	270	0
0.01	3×10^{-3}	210	−0.24
0.2	6×10^{-2}	210	−0.09
1.0	3×10^{-1}	200	−0.23

2.2. Catalyst testing

The catalytic tests of indole hydrodenitrogenation were performed in a dynamic high-pressure flow reactor equipped with a piston pump (Gilson 302) injecting the indole/cyclohexane/decane (reactant/solvent/internal standard) mixture into the hydrogen carrier gas (Air Liquide, 99.995%). Indole, cyclohexane and decane with a purity grade of 99+% were purchased from Acros Organics. The pressure in the catalytic unit was regulated using a back-pressure valve (Brooks 5866) and the gas flow rate was controlled by mass flow controllers (Brooks 5850 TR). Reactants and products were separated and analyzed on-line on an ultra 1-methyl silicone gum capillary column (50 m long and 0.33 μm of the internal diameter) installed in a Hewlett Packard GC 5890 gas chromatograph equipped with an ionization flame detector. The measurements were carried out at 573 K, under a pressure of 50 atm, the contact time varying from 0.03 to 0.7 s and the hydrocarbon to hydrogen volumetric ratio of 1/1000. Prior to the catalytic tests the catalysts were activated in pure hydrogen at 723 K for 2 h.

Kinetic modeling was based on a classic one loop network of consecutive-parallel reactions:

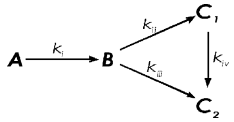

The symbolic processing and analytical integration of the resultant differential rate equations were performed using *Matematica* (Wolfram Research Inc.) and the non-linear fitting of the data was carried out using Levenberg–Marquardt method implemented in *Origin* program (Origin Lab Corp.).

3. Results and discussion

3.1. Kinetic model

There is some consensus in the literature on the generic reaction network for indole HDN [6–9]. The network consists of multiple steps of hydrogenation, hydrogenolysis, dehydrogenation and nucleophilic substitution and elimination reactions that are significantly affected by pressure, temperature, feed concentration and the catalysts as well. The reaction is initiated with hydrogenation of the heterocyclic ring in a reversible step leading to formation of indoline. This step is in thermodynamic equilibrium under most conditions. Starting from indoline the reaction diverges into pathways involving *o*-ethyloaniline (OEA) or octahydroindole (OHI) as intermediates. The early denitrogenation (EDN) route starts from OEA and going through dihydro-*o*-ethylaniline

(DHOEA) ends up with ethylbenzene (EB). The second, late denitrogenation (LDN), route occurs with hydrogenation of OEA to form *o*-ethylcyclohexylamine (OECHA) and then ethylcyclohexane (ECH) is produced as the final HDN product. Thus, the EDN and LDN pathways differ by the relative position, where the nitrogen atom removal takes place via E2 elimination, with respect to the OEA intermediate. The decisive event, triggering this process, is transformation of the carbon atom to which the NH_2 group is attached from sp^2 into sp^3 upon addition of hydrogen [10].

The two main HDN products EB and ECH can be coupled by a hydrogenation process, which was found to be kinetically significant for longer contact times. The proposed global reaction scheme (Fig. 1) that summarizes the most important steps of indole HDN was used for the analysis of the observed kinetic data. Although OECHA is a common species for both OEA and OHI pathways, in our case the distribution of products and the observed intermediates (marked in dark in Fig. 1) suggest that the OHI branch can be neglected. This remains in line with previous HDN studies over molybdenum carbides and nitrides [7,11], in contrast to sulfided bimetallic CoMo and NiMo catalysts, where the OHI pathway is usually preferred, however the key intermediate has been only scarcely observed [8,9].

The reaction scheme from Fig. 1 implies the following rate equations for the decay of indole and formation of the three most important products (OEA, EB, ECH) observed in the course of the catalytic tests.

$$r_{\mathrm{Ind}} = -\frac{\mathrm{d[Ind]}}{\mathrm{d}t} = k_1[{}^*\mathrm{Ind}][\mathrm{H}^*\mathrm{H}][\mathrm{L}^{-1}]$$

$$r_{\mathrm{OEA}} = \frac{\mathrm{d[OEA]}}{\mathrm{d}t} = \{k_1[{}^*\mathrm{Ind}] - (k_{1\mathrm{H}} + k_{1\mathrm{D}})[{}^*\mathrm{OEA}]\}[\mathrm{H}^*\mathrm{H}][\mathrm{L}^{-1}]$$

$$r_{\mathrm{EB}} = \frac{\mathrm{d[EB]}}{\mathrm{d}t} = \{k_{1\mathrm{D}}[{}^*\mathrm{OEA}] - k_3[{}^*\mathrm{EB}]\}[\mathrm{H}^*\mathrm{H}][\mathrm{L}^{-1}]$$

$$r_{\mathrm{ECH}} = \frac{\mathrm{d[ECH]}}{\mathrm{d}t} = \{k_{1\mathrm{H}}[{}^*\mathrm{OEA}] + k_3[{}^*\mathrm{EB}]\}[\mathrm{H}^*\mathrm{H}][\mathrm{L}^{-1}]$$

Taking into account the balance of the surface sites

$$[\mathrm{L}] = [{}^*] + [{}^*\mathrm{Ind}] + [\mathrm{H}^*\mathrm{H}] + [{}^*\mathrm{OEA}] + [{}^*\mathrm{ECH}] + [{}^*\mathrm{EB}] + [{}^*\mathrm{NH_3}] + \varepsilon$$

where ε stands for the residual occupied sites by the minor surface species that are kinetically insignificant, * indicates the free active sites and H*H refers to hydrogen molecule activated on one site. The amount of active sites [*] under reaction conditions is considered to be small and nearly constant. Therefore, the above equations can be expressed as

$$r_{\mathrm{Ind}} = [{}^*]^2 k_1 \mathrm{K}_{\mathrm{H_2}} p_{\mathrm{H_2}} \mathrm{K}_{\mathrm{Ind}}[\mathrm{L}^{-1}][\mathrm{Ind}] = k_{\mathrm{IND}}[\mathrm{Ind}]$$

$$r_{\mathrm{OEA}} = [{}^*]^2 \mathrm{K}_{\mathrm{H_2}} p_{\mathrm{H_2}}[\mathrm{L}^{-1}]\{\mathrm{K}_{\mathrm{Ind}}[\mathrm{Ind}] - (k_{1\mathrm{D}} + k_{1\mathrm{H}})\mathrm{K}_{\mathrm{OEA}}[\mathrm{OEA}]\} = k_{\mathrm{IND}}[\mathrm{Ind}] - (k_{\mathrm{EDN}} + k_{\mathrm{LDN}})[\mathrm{OEA}]$$

$$r_{\mathrm{EB}} = [{}^*]^2 \mathrm{K}_{\mathrm{H_2}} p_{\mathrm{H_2}}[\mathrm{L}^{-1}]\{k_{1\mathrm{D}}\mathrm{K}_{\mathrm{OEA}}[\mathrm{OEA}] - k_3\mathrm{K}_{\mathrm{EB}}[\mathrm{EB}]\} = k_{\mathrm{EDN}}[\mathrm{OEA}] - k_{\mathrm{EB}}[\mathrm{EB}]$$

$$r_{\mathrm{ECH}} = [{}^*]^2 \mathrm{K}_{\mathrm{H_2}} p_{\mathrm{H_2}}[\mathrm{L}^{-1}]\{k_{1\mathrm{H}}\mathrm{K}_{\mathrm{OEA}}[\mathrm{OEA}] + k_3\mathrm{K}_{\mathrm{EB}}[\mathrm{EB}]\} = k_{\mathrm{HYD}}[\mathrm{OEA}] + k_{\mathrm{EB}}[\mathrm{EB}]$$

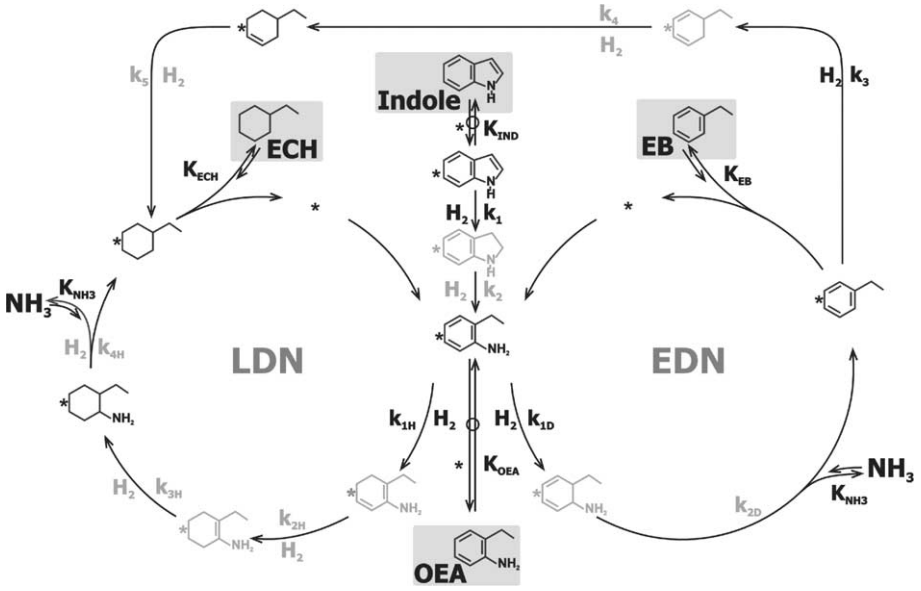

Fig. 1. The reaction network with the EDN and LDN cycles used for the kinetic modeling of the HDN of indole over bare and potassium doped Mo_2C catalysts. The species marked in dark were directly observed during the catalytic tests, whereas in shadowed boxes are those explicitly included in the kinetic model. The symbol ⇔ indicates quasi-equilibrium.

where [*] is equal to:

$$[^*] = \frac{[L]}{[1] + K_{Ind}[Ind] + K_{H_2} p_{H_2} + K_{OEA}[OEA] + K_{ECH}[ECH] + K_{EB}[EB] + K_{NH_3}[NH_3]}$$

Thus, the parameters to be experimentally determined are the apparent rate constants k_{IND} (indole hydrogenation), k_{EDN} (OEA hydrogenation in EDN cycle), k_{LDN} (OEA hydrogenation in the LDN cycle) and k_{EB} (EB hydrogenation to ECH).

3.2. Kinetic results

The kinetic results (molar distribution vs. contact time) as a function of potassium loading are shown in Fig. 2a–d. The curves resulting from the kinetic model were successfully fitted to the experimental points with the R^2 coefficient better than 0.99 for 0, 0.01, 0.2 wt.% of potassium. However, for 1 wt.% it was equal to 0.94 because the experimental points were more scattered. The observed curves are typical for a network of consecutive-parallel reactions. Except for the highest potassium content the evolution of the kinetic data is essentially similar. Whereas for lower potassium loadings the principal product of indole HDN is ethylcyclohexane in the case of the sample containing 1 wt.% of potassium this product is largely suppressed and ethylbenzene formation becomes dominant. A more in-depth insight into the effect of potassium on the reaction course can be inferred from the values of the apparent rate constants, which are summarized in Table 2.

The rate constants, k_{IND} and k_{EDN} exhibit a similar, non-monotonous dependence on the potassium loading. These rate constants are associated with the EDN cycle and characterize the hydrogenation reactions of indole to EB via the OEA intermediate. A similar behavior exhibits also the k_{EB} constant linked with hydrogenation of EB to ECH, which couples the EDN and LDN cycles. In contrast, the k_{LDN} constant that gauges the parallel transformation of OEA to ECH monotonously decreases upon addition of the K promoter. It is worth to notice that the first three rate constants followed the changes in the work function of the catalysts (Table 1), implying that the electronic factor is probably of primary importance for the EDN pathway. Indeed, a more detailed study on the interaction between an indole molecule and the Mo_2C surface revealed that even a small shift (~0.2 eV) in the work function can largely

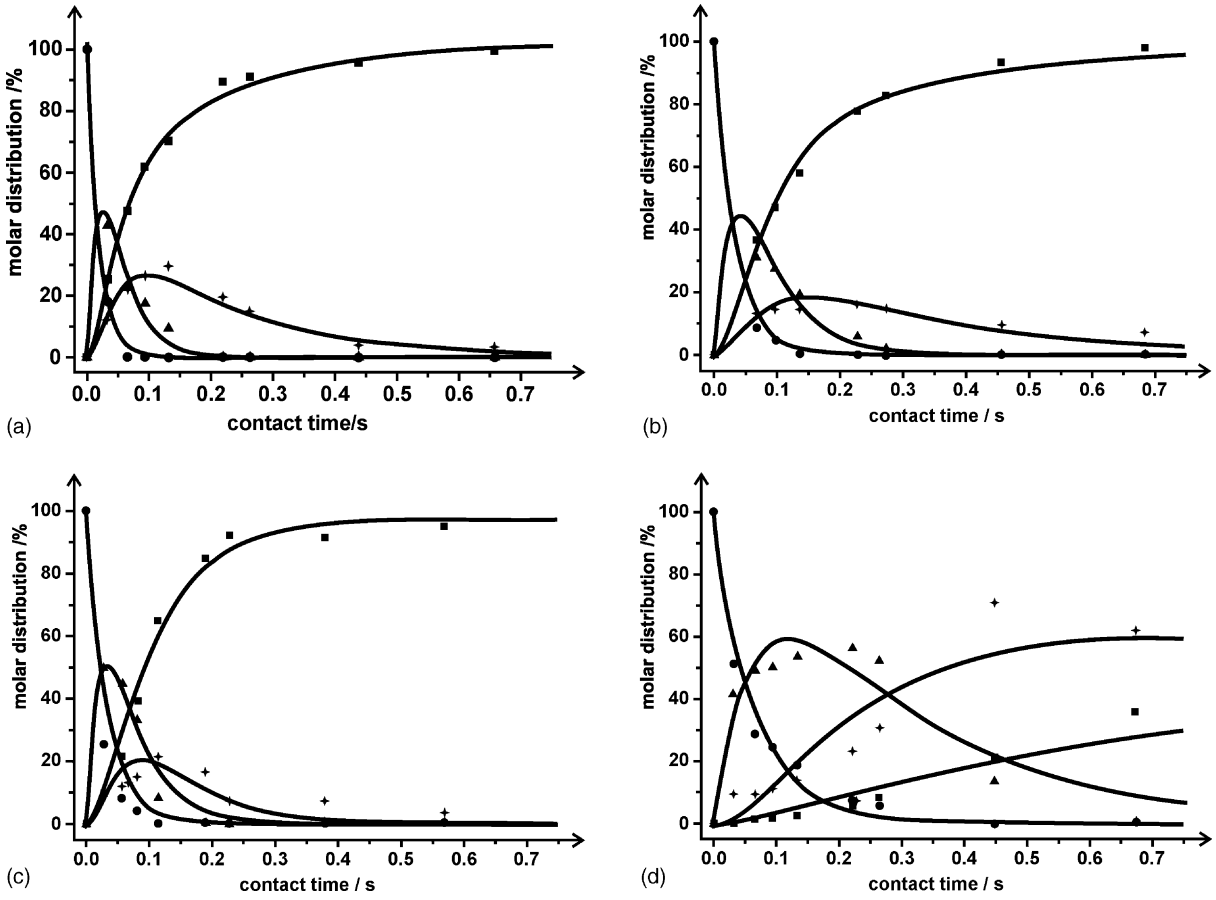

Fig. 2. Reactant and products (●: indole, ▲: OEA, ■: ECH, ✦ EB) distribution vs. contact time for the HDN of indole over the Mo_2C catalysts for: (a) 0, (b) 3×10^{-3}, (c) 6×10^{-2}, and (d) 3×10^{-1} of potassium coverage. The lines were obtained by fitting the kinetic curves derived from the model to the experimental data.

Table 2
Apparent rate constants for the HDN of indole over K-doped Mo_2C catalysts determined from the fitting of the kinetic model to the experimental data

Surface coverage	k_{IND} (s^{-1})	k_{EDN} (s^{-1})	k_{LDN} (s^{-1})	k_{EB} (s^{-1})	k_{EDN}/k_{LDN}	$\left(\frac{[EB]}{[ECH]}\right)_{\tau=0.5}$
0	50.61 ± 2.87	11.78 ± 0.84	18.10 ± 0.91	5.22 ± 0.54	0.65 ± 0.08	0.05
3×10^{-3}	29.60 ± 2.16	5.50 ± 0.58	13.32 ± 0.75	3.65 ± 0.64	0.41 ± 0.07	0.08
6×10^{-2}	44.38 ± 3.30	10.17 ± 1.55	9.59 ± 1.53	13.42 ± 2.90	1.06 ± 0.33	∼0.0
3×10^{-1}	14.76 ± 1.16	3.26 ± 0.39	0.75 ± 0.39	0.43 ± 0.36	4.37 ± 2.67	2.7

influence indole activation upon adsorption and, therefore, control the rate of its hydrodenitrogenation [4].

The last two columns in Table 2 show the ratios of rate constants k_{EDN}/k_{LDN} and of [EB]/[ECH] for the contact time $\tau = 0.5$ s, respectively. Disregarding some irregularities the general tendency is that both ratios increase with the K-loading. In terms of the kinetic model this indicates that the addition of potassium favors the EDN cycle in comparison to the LDN cycle (Fig. 1) that is considerably slowed down. Apparently, the presence of potassium favors the attack by atomic hydrogen on the C_1=C_2 double bond of the OEA intermediate, while on the bare Mo_2C the hydrogenation preferentially occurs at the C_3=C_4 and C_5=C_6 double bonds.

4. Conclusions

The model based on two coupled cycles, with early and late denitrogenation steps, accounts well for the observed kinetic curves of indole HDN catalyzed by K-doped Mo_2C. Potassium strongly influences the rate constants of all kinetically significant processes and by slowing down the cycle with the late denitrogenation step the selectivity changes to aromatics.

Acknowledgements

This work was done within the Research Project 3T09A17219 sponsored by Polish Committee for Scientific Research. The authors acknowledge also the French–Polish cooperation within the program Jumelage “Carbonaceous and Catalytic Materials for Environment”.

References

[1] S.T. Oyama, Catal. Today 15 (1992) 179.
[2] L.I. Johansson, Surf. Sci. Rep. 21 (1995) 177.
[3] A. Kotarba, G. Adamski, Z. Sojka, S. Witkowski, G. Djega-Mariadassou, Stud. Surf. Sci. Catal. 130 (2000) 485.
[4] A. Kotarba, G. Adamski, W. Piskorz, Z. Sojka, C. Sayag, G. Djéga-Mariadassou, J. Phys. Chem. B 108 (2004) 2885.
[5] R. Kojami, K. Aika, Appl. Catal. A: General 219 (2001) 141.
[6] H. Abe, A.T. Bell, Catal. Lett. 18 (1993) 1.
[7] K. Miga, K. Stañczyk, C. Sayag, D. Brodzki, G. Djéga-Mariadassou, J. Catal. 183 (1999) 63.
[8] S.C. Kim, F.E. Massoth, Ind. Eng. Chem. Res. 39 (2000) 1705.
[9] A. Bunch, L. Zhang, G. Karkas, U.S. Ozkan, Appl. Catal. A: General 190 (2000) 51, and the references therein.
[10] P. Da Costa, C. Potvin, J.-M. Manoli, J.L. Lemberton, G. Perot, G. Djega Mariadassou, J. Mol, Catal. A: Chemical 184 (2002) 323.
[11] A. Szymańska, M. Lewandowski, C. Sayag, G. Djega-Mariadassou, J. Catal. 218 (2003) 24.